

Alma Mater Studiorum Università di Bologna
Archivio istituzionale della ricerca

Electrogenerated Chemiluminescence with Peroxydisulfate as a Coreactant Using Boron Doped Diamond Electrodes

This is the final peer-reviewed author's accepted manuscript (postprint) of the following publication:

Published Version:

Fiorani, A., Irkham, n., Valenti, G., Paolucci, F., Einaga, Y. (2018). Electrogenerated Chemiluminescence with Peroxydisulfate as a Coreactant Using Boron Doped Diamond Electrodes. ANALYTICAL CHEMISTRY, 90(21), 12959-12963 [10.1021/acs.analchem.8b03622].

Availability:

This version is available at: <https://hdl.handle.net/11585/654909> since: 2019-01-14

Published:

DOI: <http://doi.org/10.1021/acs.analchem.8b03622>

Terms of use:

Some rights reserved. The terms and conditions for the reuse of this version of the manuscript are specified in the publishing policy. For all terms of use and more information see the publisher's website.

This item was downloaded from IRIS Università di Bologna (<https://cris.unibo.it/>).
When citing, please refer to the published version.

(Article begins on next page)

This is the final peer-reviewed accepted manuscript of:

Andrea Fiorani, Irkham, Giovanni Valenti, Francesco Paolucci, and Yasuaki Einaga
Electrogenerated Chemiluminescence with Peroxydisulfate as a Coreactant Using
Boron Doped Diamond Electrodes

***Analytical Chemistry* 2018 90 (21), 12959-12963**

The final published version is available online at:
<https://doi.org/10.1021/acs.analchem.8b03622>

Rights / License:

The terms and conditions for the reuse of this version of the manuscript are specified in the publishing policy. For all terms of use and more information see the publisher's website.

This item was downloaded from IRIS Università di Bologna (<https://cris.unibo.it/>)

When citing, please refer to the published version.

Electrogenerated Chemiluminescence with Peroxydisulfate as a Coreactant Using Boron Doped Diamond Electrodes

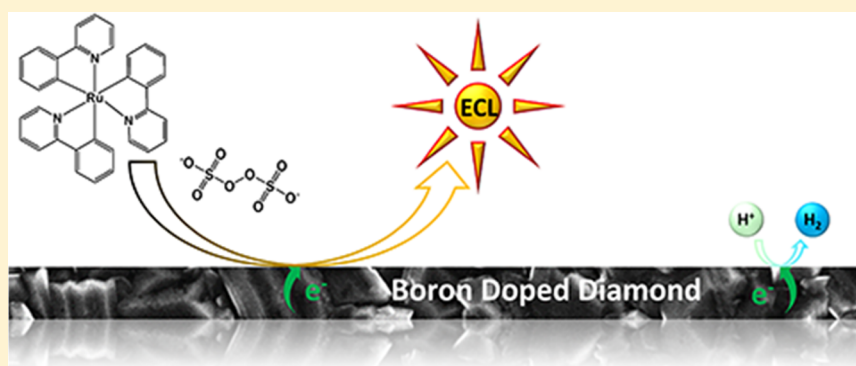
Andrea Fiorani,[†] Irkham,[†] Giovanni Valenti,^{‡,§} Francesco Paolucci,^{‡,§} and Yasuaki Einaga^{*,†,§}

[†]Department of Chemistry, Keio University, 3-14-1 Hiyoshi, Yokohama 223-8522, Japan

[‡]Department of Chemistry "G. Ciamician", University of Bologna, Via Selmi, 2, 40126 Bologna, Italy

[§]JST-ACCEL, 3-14-1 Hiyoshi, Yokohama 223-8522, Japan

[#]ICMATE-CNR Bologna Associate Unit, University of Bologna, 40126, Bologna, Italy



ABSTRACT: We report on the use of boron doped diamond electrodes for the electrochemiluminescence (ECL) of the coreactant peroxydisulfate and the luminophore ruthenium(II)-tris(2,2'-bipyridine). Compared to common electrode materials (i.e., Pt, Au, glassy carbon), boron doped diamond has a large overpotential for the evolution of hydrogen in aqueous electrolyte solutions. This intrinsic feature enables reductive-oxidation ECL with peroxydisulfate to be obtained without interference from hydrogen evolution and with high reproducible signals and stable emission. We investigated the effects of the peroxydisulfate concentration and the pH on the ECL emission to find the optimal conditions for enhancing the signal.

Electrogenerated chemiluminescence (ECL) is a complex phenomenon involving light emission triggered by electrochemical reactions at an electrode surface.¹ Despite the emission being generated from an excited state by a homogeneous electron transfer in solution, ECL is highly dependent on the electrode material, since this may have a large effect on the heterogeneous electron transfer that ignites ECL.² The combination of electrode material and solvent is also extremely important, fixing the available potential window.

Nowadays, aqueous solutions are prominent in analytical ECL applications,³⁻⁵ and thanks to the optimal signal-to-noise ratio, ECL is a leading technique in bioanalysis, also in very complex matrixes such as urine and serum.⁶⁻⁸ On the other hand, organic solvents retain a useful application in luminophores characterization,⁹⁻¹³ emitting devices,¹⁴⁻¹⁸ and mixed annihilation.^{19,20} However, water oxidation and hydrogen evolution hampers the possibilities of ECL. This drawback has been overcome by the use of a coreactant, a sacrificial molecule that allows the generation of ECL within the water potential window. This dependency was investigated to a great extent for many ECL coreactant/electrode material systems² and mainly for the oxidative-reduction ECL mechanism of Ru(bpy)₃²⁺/tri-*n*-propylamine.^{21,22}

For example, ECL for the Ru(bpy)₃²⁺/tri-*n*-propylamine system has oxidation potentials of 1.27 and 1.12 V (vs NHE), respectively, which are comparable or lower than the potential for water oxidation, 1.23 V (vs NHE).

On the other hand, ECL working with a cathodic current by the reductive-oxidation coreactant mechanism can be easily hampered by hydrogen evolution.²³ In fact this approach is used mainly in organic solvents,^{24,25} although coreactant ECL has been reported for water solutions with carbon paste electrodes and glassy carbon electrodes, for peroxydisulfate²⁶⁻²⁸ and hydrogen peroxide.²⁹ In this context, the electrode material can play a crucial role by shifting the hydrogen evolution to a higher potential, while retaining the reduction potentials for the ECL reactants.^{2,30}

Boron doped diamond electrodes (BDD) have a wider potential window in water compared to common electrode materials, with a high overpotential for hydrogen evolution,^{31,32} thus are highly suited to reductive-oxidation ECL in water. Moreover, the properties of BDD electrodes are tunable

by the amount of sp^2 carbon^{33,34} and various surface functionalizations are easily accessible.^{35–37} However, nowadays, ECL applications of the reductive-oxidation of peroxydisulfate are performed at GC or carbon based electrodes^{38–44} that limit the sensitivity of this ECL system.

Here, we report on the electrogenerated chemiluminescence of the $\text{Ru}(\text{bpy})_3^{2+}$ /peroxydisulfate system using boron doped diamond electrodes. We examine a wide range of peroxydisulfate concentrations and the effect of the pH value.

EXPERIMENTAL SECTION

Materials. $\text{Ru}(\text{bpy})_3\text{Cl}_2 \cdot 6\text{H}_2\text{O}$, NaClO_4 , $\text{Na}_2\text{S}_2\text{O}_8$, KH_2PO_4 , and Na_2HPO_4 were purchased from Wako Pure Chemical (JP) and used without further purification. A phosphate buffer (PB) was prepared at pH 6.8 using KH_2PO_4 and Na_2HPO_4 only. Pure double distilled water (ddw), conductivity $<18 \text{ M}\Omega$, was obtained from a SimplyLab water system (DIRECT-Q3 UV, Millipore).

Preparation of BDD. The BDD films were deposited on a silicon (111) wafer using a microwave plasma-assisted chemical vapor deposition (MPCVD) system (CORNES Technologies/ASTeX–5400). Trimethoxyborane and acetone were used as the boron and carbon sources, respectively, with an atomic ratio of $B/C = 1\%$ ($B \approx 2 \times 10^{21}/\text{cm}^3$). The surface morphology of the BDD was examined using a field emission scanning electron microscope (FESEM, JEOL JSM-7600F). Raman spectra were recorded with an Acton SP2500 (Princeton Instruments) with an excitation wavelength of 532 nm from a green laser diode at ambient temperature (Figure S1).

Electrochemical Measurements. All the ECL measurements were conducted with a conventional three-electrode system in a PTFE cell (2.5 cm^3) with a 1% BDD, a Pt or glassy carbon (GC) working electrodes (0.635 cm^2), counter platinum spiral, and Ag/AgCl (saturated KCl) reference electrode (all potentials throughout the text are referred to this electrode). The electrodes were connected to an Autolab PGSTAT302N (Metrohm).

The ECL signal was measured with a photomultiplier tube (PMT, Hamamatsu R928) placed at a fixed height from the electrochemical cell, inside a dark box. A high voltage power supply socket assembly with a transimpedance amplifier (Hamamatsu C6271) was used to supply 500 V to the PMT, using an external trigger connection to the Autolab DAC module. Light/current/voltage curves were recorded by collecting the amplified PMT output signal with the ADC module of the Autolab. ECL spectra were collected by a SEC2000 Spectra system UV–visible spectrophotometer (ALS Co., JP), by means of an optical fiber on top of the electrochemical cell.

The BDD electrode was cleaned by sonication in isopropanol for 5 min, rinsed in ddw, and dried in a stream of nitrogen. Prior to each ECL measurement, the BDD surface was pretreated electrochemically to guarantee reproducibility, by performing 10 voltammetric cycles between -2.0 and 2.0 V followed by 10 cycles between 0 and -2.0 V in a 0.1 M NaClO_4 solution at a scan rate 0.3 V/s . The GC (Tokai Carbon, JP) and Pt (Nilaco Co., JP) electrodes were cleaned with $0.5 \mu\text{m}$ alumina powder on cloth tape, then sonicated in ddw for 5 min, rinsed in ddw, and dried in a nitrogen stream.

RESULTS AND DISCUSSION

First, we investigated the ECL of $\text{Ru}(\text{bpy})_3^{2+}$ /peroxydisulfate at a BDD electrode by cyclic voltammetry and we compared this with the results obtained using Pt and GC electrodes (Figure 1). However, there were no ECL signals with the Pt

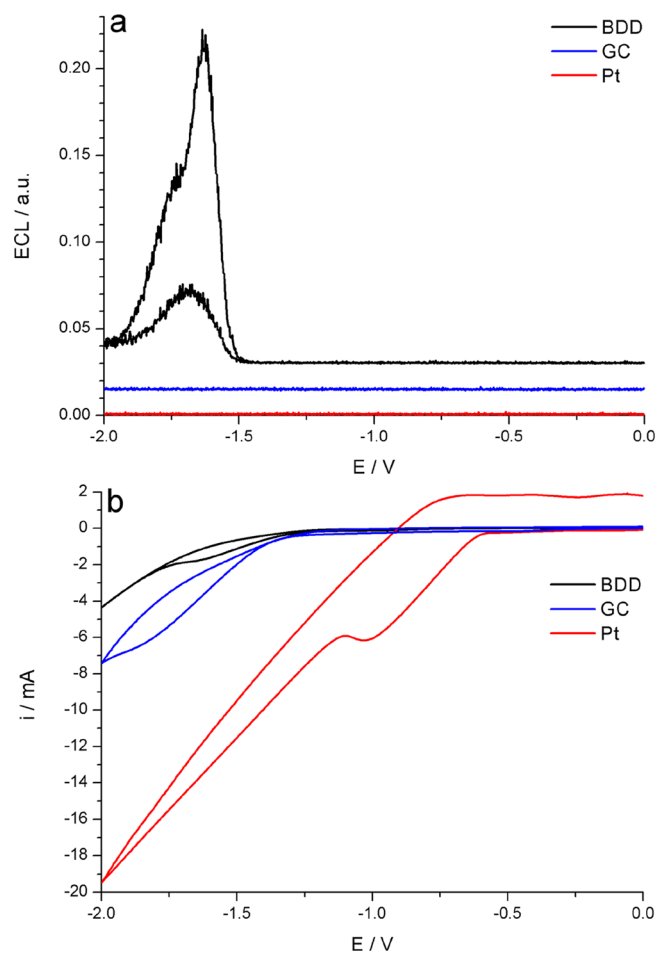


Figure 1. Comparison of ECL (a) and CV (b) with BDD (black), GC (blue), and Pt (red) electrodes for $10 \mu\text{M}$ $\text{Ru}(\text{bpy})_3^{2+}$ and $100 \mu\text{M}$ $\text{S}_2\text{O}_8^{2-}$ in 200 mM PB. The scan rate is 100 mV/s and the pH 6.8. In part a, the curves are shifted for clarity.

and GC electrodes, though there was detectable ECL emission for $\text{Ru}(\text{bpy})_3^{2+}$ /peroxydisulfate with the GC electrode when the concentration was 5 times higher (Figure S2). In contrast, the ECL signal from the BDD electrode was high. The rate of hydrogen evolution, which is related to the cathodic current ($\text{BDD} < \text{GC} \ll \text{Pt}$), adversely affects the ECL emission, preventing light detection, and hindering the reduction of $\text{Ru}(\text{bpy})_3^{2+}$ and peroxydisulfate in favor of proton reduction. The higher overpotential for proton reduction at BDD, compared to GC and Pt, makes diamond electrodes far superior for reductive-oxidation ECL in aqueous solutions.

The ECL signal starts at -1.47 V corresponding to $\text{Ru}(\text{bpy})_3^{2+}/\text{Ru}(\text{bpy})_3^+$ ($E^0 = -1.46 \text{ V}$), with a steep rise at -1.5 V and a maximum at -1.6 V . The ECL with the GC electrode shows similar potentials; however, a higher concentration of $\text{Ru}(\text{bpy})_3^{2+}$ /peroxydisulfate was needed (Figure S2), similar to that used by Choi and Bard where $\text{Ru}(\text{bpy})_3^{2+}$ was in the millimolar concentration range.²⁹ The BDD electrode has high ECL stability with repetitive cycling

(Figure S3), even though a decrease in the emission is observed after the first cycle, likely due to surface modification after the potential scan,^{31,32,37} and commonly observed for the ECL emission.^{21,30}

The ECL with the BDD electrode features two emission peaks at different potentials. In the ECL plot, $\text{Ru}(\text{bpy})_3^{2+}$ is identified as the emitting species, with a maximum at 610 nm for -1.6 V, together with a second peak at 630 nm at a potential of -1.7 V (Figure 2 and Figure S4).

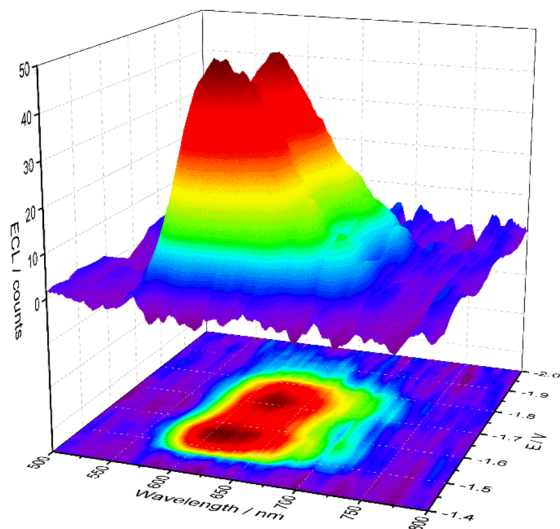
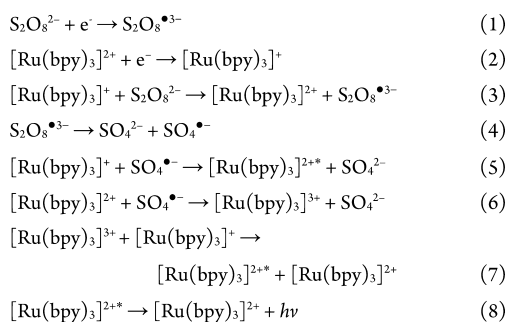


Figure 2. 3D surface plot of ECL spectrum with a BDD electrode as a function of applied potential. The solution is $10 \mu\text{M}$ $\text{Ru}(\text{bpy})_3^{2+}$ and $100 \mu\text{M}$ $\text{S}_2\text{O}_8^{2-}$ in 200 mM PB. The scan rate is 100 mV/s and the pH 6.8 . Integration time for the spectrum: 200 ms .

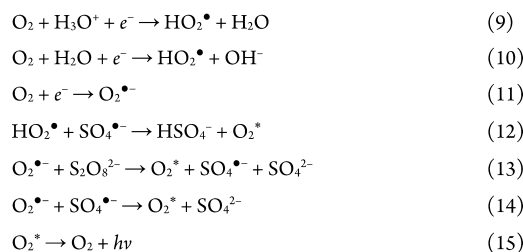
The ECL underlying the first peak is described by reactions 1–8 in Scheme 1, the mechanism of reductive-oxidation ECL for $\text{Ru}(\text{bpy})_3^{2+}$ /peroxydisulfate.^{23,30,45}

Scheme 1



The second ECL peak, which is a shoulder on the main peak, is cautiously ascribed to emitting oxygen species generated by peroxydisulfate (Scheme 2, reactions 9–15).⁴⁶ This ECL emission has previously been demonstrated for electrolysis in an aqueous solution of peroxydisulfate, where excited oxygen species such as $^1\text{O}_2$, $^1(\text{O}_2)_2$, and $^3(\text{O}_2)_2$ were generated.^{26,47,48} The emission is quite broad, with a range of wavelengths from 500 to 700 nm . In particular, a peak at 634 nm can be assigned to the chemiluminescent reaction $(\text{O}_2(^1\Delta_g))_2 \rightarrow (\text{O}_2(^3\Sigma_g^-))_2$,^{49–52} which is very close and can be ascribed to the observed ECL peak of 630 nm .

Scheme 2



The ECL response as a function of the peroxydisulfate concentration was assessed in the range from $1 \mu\text{M}$ to 100 mM (Figure 3). A linear increase was found at low peroxydisulfate

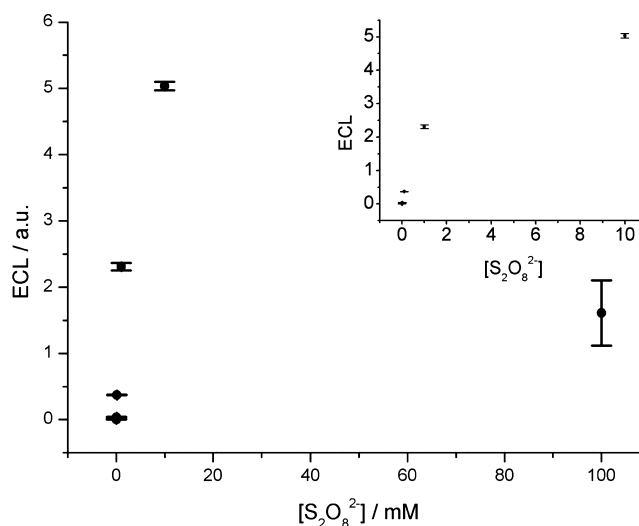
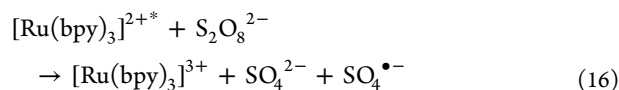


Figure 3. Integrated ECL emission with a BDD electrode as a function of $\text{S}_2\text{O}_8^{2-}$ concentration, from $1 \mu\text{M}$ to 100 mM , by cyclic voltammetry. Inset: magnification of ECL response from $1 \mu\text{M}$ to 10 mM . Solution, $10 \mu\text{M}$ $\text{Ru}(\text{bpy})_3^{2+}$ in 200 mM PB; scan rate, 100 mV/s ; pH, 6.8 .

concentrations (1 – $100 \mu\text{M}$), resulting in $\text{LOD} = 0.5 \mu\text{M}$ and $\text{LOQ} = 1 \mu\text{M}$ (Figure S5). The maximum emission occurs at 10 mM , while at 100 mM , the emission is much less.

This trend in ECL emission for peroxydisulfate has been observed previously,^{23,45} and it reflects the oxidative quenching of peroxydisulfate on the excited state of $\text{Ru}(\text{bpy})_3^{2+}$ by reaction 16, with a quenching rate constant (k_q) and an electron transfer rate constant (k_{et}) within the excited-state ion pair ($\text{Ru}(\text{bpy})_3^{2+*}|\text{S}_2\text{O}_8^{2-}$) of $9.8 \times 10^8 \text{ M}^{-1} \text{ s}^{-1}$ and $4.2 \times 10^8 \text{ s}^{-1}$, respectively.⁵³ Interestingly, we found new evidence for ECL emission for solutions with a $\text{Ru}(\text{bpy})_3^{2+}$ /peroxydisulfate ratio down to $1/1000$ ($10 \mu\text{M}/10 \text{ mM}$), while previous data from White et al.²³ reported a value of $1/20$ and those from Yamazaki-Nishida et al.²⁷ gave $1/200$. This increases the range of persulfate concentrations available that can be used profitably without interference by oxidative quenching, which will enable a wider range of $\text{Ru}(\text{bpy})_3^{2+}$ detection.



We observed, not only changes in the ECL intensity with concentration but also in the relative intensities of the first and second peaks (Figure 4). While the first peak intensity

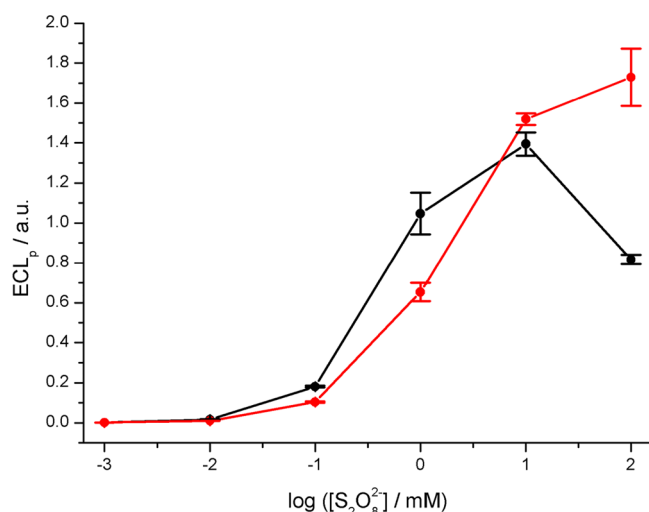
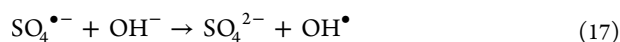


Figure 4. Comparison of ECL peak intensity for first (black) and second (red) peaks as a function of peroxydisulfate concentration. The scan rate is 100 mV/s and the pH 6.8.

increases with concentration, through a maximum to a quenched emission, resembling the integrated ECL of Figure 3, the second peak intensity increases with increasing peroxydisulfate concentration. These results support the assignment of first peak to ECL from $\text{Ru}(\text{bpy})_3^{2+}$ /peroxydisulfate (Scheme 1) and the second peak to O_2 /peroxydisulfate (Scheme 2).

Since the main drawback of reductive-oxidation processes in aqueous solutions is the evolution of hydrogen, we assessed the effect of pH on the ECL intensity by cyclic voltammetry, from pH 2 to 9 (Figure 5). Even at higher concentrations of peroxydisulfate (1 mM), the trend is similar (Figure S6).

A decrease in pH results in two distinctive effects, an increase in the ECL emission and a shift to negative potentials of the ECL peak (Figure 5b). The ECL decrease from pH 4 to 9 can be ascribed to the quenching effect of hydroxyl ions on sulfate radical anions, with a rate constant of $6.5 \pm 1.0 \times 10^7 \text{ M}^{-1} \text{ s}^{-1}$ (reaction 17).⁵⁴



Although the cathodic current for hydrogen evolution increases (Figure S7), this is not a limiting factor that hinders the ECL emission, at least until pH 4, while for pH 3 the ECL decreases and is completely turned off at pH 2. However, this might be responsible for the shift in potential of the ECL peak to more negative values with decreasing pH. The decrease in ECL due to hydrolysis of the peroxydisulfate is negligible, since the rate constants for the hydrogen ion catalyzed thermal decomposition of peroxydisulfate are very low at room temperature.⁵⁵ A similar trend in ECL emission was previously observed,⁵⁶ although by using ruthenium bipyrazine ($\text{Ru}(\text{bpz})_3^{2+}/\text{Ru}(\text{bpz})_3^+ E^0 = -0.77 \text{ V}$),⁵⁷ which can be protonated at low pH, in that case decreasing the ECL emission.

CONCLUSIONS

Here, we report on the superiority of BDD as an electrode material for ECL from the coreactant peroxydisulfate in water. Nowadays, many ECL applications with peroxydisulfate are performed using GC or carbon based electrodes; however, BDD can effectively increase the ECL emission for peroxydisulfate, suppressing the hydrogen evolution and

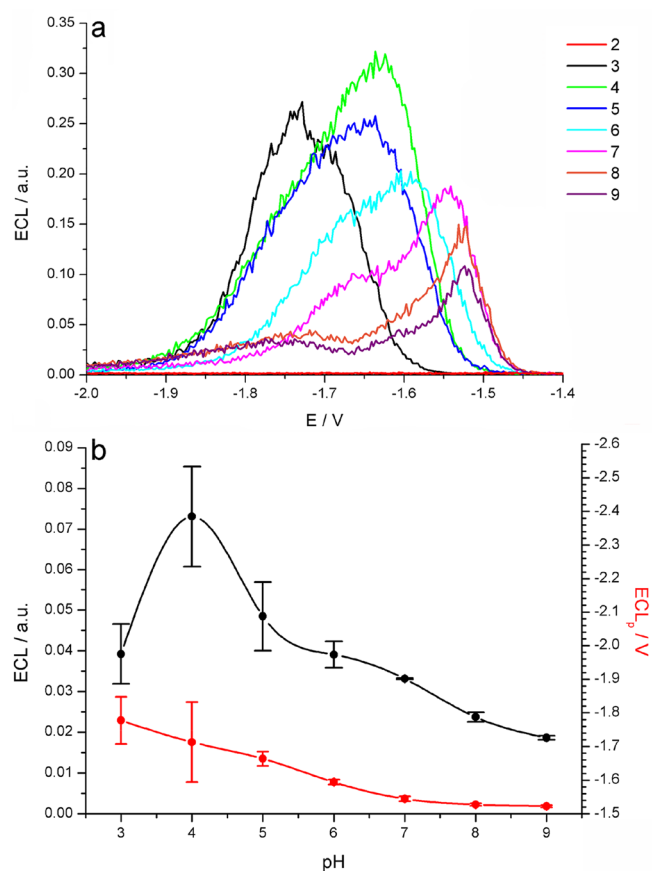


Figure 5. (a) ECL by CV for 10 μM $\text{Ru}(\text{bpy})_3^{2+}$ and 100 μM $\text{S}_2\text{O}_8^{2-}$ in 200 mM PB, for pH 2 to 9. The scan rate is 100 mV/s. (b) Integrated ECL (black) and ECL peak potential (red) as functions of pH.

increasing the stability, leading to higher sensitivity and lower detection limits, which cannot be reached using GC electrodes. ECL can be performed over a wide range of peroxydisulfate concentrations and pH values, thus meeting the experimental requirements of many applications. The reported results, besides contributing to a better understanding of the mechanisms operating in the generation of ECL, also pave the way for the development of highly efficient ECL for ultrasensitive bioanalysis.

ASSOCIATED CONTENT

Supporting Information

The Supporting Information is available free of charge on the ACS Publications website at DOI: 10.1021/acs.anal-chem.8b03622.

BDD Raman spectra and SEM micrographs, ECL at GC, ECL spectra at selected potentials, peroxydisulfate LOD and LOQ, and ECL and cathodic currents for pH variation (PDF)

Notes

The authors declare no competing financial interest.

ACKNOWLEDGMENTS

G.V. and F.P. thank the University of Bologna, Italian Ministero dell'Istruzione, Università e Ricerca (MIUR-Project) and FARB, Fondazione Cassa di Risparmio in Bologna.

REFERENCES

- (1) Fiorani, A.; Valenti, G.; Iurlo, M.; Marcaccio, M.; Paolucci, F. *Curr. Opin. Electrochem.* **2018**, *8*, 31–38.
- (2) Valenti, G.; Fiorani, A.; Li, H.; Sojic, N.; Paolucci, F. *ChemElectroChem* **2016**, *3*, 1990–1997.
- (3) Hesari, M.; Ding, Z. *J. Electrochem. Soc.* **2016**, *163*, H3116–H3131.
- (4) Richter, M. M. *Chem. Rev.* **2004**, *104*, 3003–3036.
- (5) Miao, W. *Chem. Rev.* **2008**, *108*, 2506–2553.
- (6) Valenti, G.; Rampazzo, E.; Biavardi, E.; Villani, E.; Fracasso, G.; Marcaccio, M.; Bertani, F.; Ramarli, D.; Dalcanele, E.; Paolucci, F.; Prodi, L. *Faraday Discuss.* **2015**, *185*, 299–309.
- (7) Li, L.; Chen, Y.; Zhu, J.-J. *Anal. Chem.* **2017**, *89*, 358–371.
- (8) Liu, Z.; Qi, W.; Xu, G. *Chem. Soc. Rev.* **2015**, *44*, 3117–3142.
- (9) Valenti, G.; Fiorani, A.; Di Motta, S.; Bergamini, G.; Gingras, M.; Ceroni, P.; Negri, F.; Paolucci, F.; Marcaccio, M. *Chem. - Eur. J.* **2015**, *21*, 2936–2947.
- (10) Hsu, C. W.; Longhi, E.; Sinn, S.; Hawes, C. S.; Young, D. C.; Kruger, P. E.; De Cola, L. *Chem. - Asian J.* **2017**, *12*, 1649–1658.
- (11) Hesari, M.; Barbon, S. M.; Mendes, R. B.; Staroverov, V. N.; Ding, Z.; Gilroy, J. B. *J. Phys. Chem. C* **2018**, *122*, 1258–1266.
- (12) Kapturkiewicz, A. *Anal. Bioanal. Chem.* **2016**, *408*, 7013–7033.
- (13) Li, H.; Voci, S.; Wallabregue, A.; Adam, C.; Labrador, G. M.; Duwald, R.; Delgado, I. H.; Pascal, S.; Bosson, J.; Lacour, J.; Bouffier, L.; Sojic, N. *ChemElectroChem* **2017**, *4*, 1750–1756.
- (14) Horiuchi, T.; Niwa, O.; Hatakenaka, N. *Nature* **1998**, *394*, 659–661.
- (15) Nobeshima, T.; Nakakomi, M.; Nakamura, K.; Kobayashi, N. *Adv. Opt. Mater.* **2013**, *1*, 144–149.
- (16) Tsuneyasu, S.; Ichihara, K.; Nakamura, K.; Kobayashi, N. *Phys. Chem. Chem. Phys.* **2016**, *18*, 16317–16324.
- (17) Tsuneyasu, S.; Ichikawa, T.; Nakamura, K.; Kobayashi, N. *ChemElectroChem* **2017**, *4*, 1731–1735.
- (18) Kong, S. H.; Lee, J. I.; Kim, S.; Kang, M. S. *ACS Photonics* **2018**, *5*, 267–277.
- (19) Kerr, E.; Doeven, E. H.; Barbante, G. J.; Hogan, C. F.; Bower, D. J.; Donnelly, P. S.; Connell, T. U.; Francis, P. S. *Chem. Sci.* **2015**, *6*, 472–479.
- (20) Kerr, E.; Doeven, E. H.; Barbante, G. J.; Hogan, C. F.; Hayne, D. J.; Donnelly, P. S.; Francis, P. S. *Chem. Sci.* **2016**, *7*, 5271–5279.
- (21) Zu, Y.; Bard, A. J. *Anal. Chem.* **2000**, *72*, 3223–3232.
- (22) Zu, Y.; Bard, A. J. *Anal. Chem.* **2001**, *73*, 3960–3964.
- (23) White, H. S.; Bard, A. J. *J. Am. Chem. Soc.* **1982**, *104*, 6891–6895.
- (24) Valenti, G.; Bruno, C.; Rapino, S.; Fiorani, A.; Jackson, E. A.; Scott, L. T.; Paolucci, F.; Marcaccio, M. *J. Phys. Chem. C* **2010**, *114*, 19467–19472.
- (25) Kudruk, S.; Villani, E.; Polo, F.; Lamping, S.; Körsen, M.; Arlinghaus, H. F.; Paolucci, F.; Ravoo, B. J.; Valenti, G.; Rizzo, F. *Chem. Commun.* **2018**, *54*, 4999–5002.
- (26) Yao, W.; Wang, L.; Wang, H.; Zhang, X. *Electrochim. Acta* **2008**, *54*, 733–737.
- (27) Yamazaki-Nishida, S.; Harima, Y.; Yamashita, K. *J. Electroanal. Chem. Interfacial Electrochem.* **1990**, *283*, 455–458.
- (28) Yamashita, K.; Yamazaki-Nishida, S.; Harima, Y.; Segawa, A. *Anal. Chem.* **1991**, *63*, 872–876.
- (29) Choi, J.-P.; Bard, A. J. *Anal. Chim. Acta* **2005**, *541*, 141–148.
- (30) Villani, E.; Valenti, G.; Marcaccio, M.; Mattarozzi, L.; Barison, S.; Garoli, D.; Cattarin, S.; Paolucci, F. *Electrochim. Acta* **2018**, *277*, 168–175.
- (31) Einaga, Y. *J. Appl. Electrochem.* **2010**, *40*, 1807–1816.
- (32) Cobb, S. J.; Ayres, Z. J.; Macpherson, J. V. *Annu. Rev. Anal. Chem.* **2018**, *11*, 463–484.
- (33) Watanabe, T.; Honda, Y.; Kanda, K.; Einaga, Y. *Phys. Status Solidi A* **2014**, *211*, 2709–2717.
- (34) Ayres, Z. J.; Newland, J. C.; Newton, M. E.; Mandal, S.; Williams, O. A.; Macpherson, J. V. *Carbon* **2017**, *121*, 434–442.
- (35) Yamamoto, T.; Akahori, M.; Natsui, K.; Saitoh, T.; Einaga, Y. *Carbon* **2018**, *130*, 350–354.
- (36) Ayres, Z. J.; Borrell, A. J.; Newland, J. C.; Newton, M. E.; Macpherson, J. V. *Anal. Chem.* **2016**, *88*, 974–980.
- (37) McCreery, R. L. *Chem. Rev.* **2008**, *108*, 2646–2687.
- (38) Russell, R.; Stewart, A. J.; Dennany, L. *Anal. Bioanal. Chem.* **2016**, *408*, 7129–7136.
- (39) Cao, J.-T.; Liu, F.-R.; Hou, F.; Peng, J.; Ren, S.-W.; Liu, Y.-M. *Analyst* **2018**, *143*, 3702.
- (40) Tian, K.; Nie, F.; Luo, K.; Zheng, X.; Zheng, J. *J. Electroanal. Chem.* **2017**, *801*, 162–170.
- (41) Lei, Y.-M.; Wen, R.-X.; Zhou, J.; Chai, Y.-Q.; Yuan, R.; Zhuo, Y. *Anal. Chem.* **2018**, *90*, 6851–6858.
- (42) Wu, F.; Feng, Y.; Chi, Y. *J. Electroanal. Chem.* **2016**, *779*, 47–54.
- (43) Guo, W.; Zhang, A.; Zhang, X.; Huang, C.; Yang, D.; Jia, N. *Anal. Bioanal. Chem.* **2016**, *408*, 7173–7180.
- (44) Wang, H.; Pu, G.; Devaramani, S.; Wang, Y.; Yang, Z.; Li, L.; Ma, X.; Lu, X. *Anal. Chem.* **2018**, *90*, 4871–4877.
- (45) Irkham; Watanabe, T.; Fiorani, A.; Valenti, G.; Paolucci, F.; Einaga, Y. *J. Am. Chem. Soc.* **2016**, *138*, 15636–15641.
- (46) Reshetnyak, O. V.; Koval'chuk, E. P. *Electrochim. Acta* **1998**, *43*, 465–469.
- (47) Reshetnyak, O. V.; Koval'chuk, E. P.; Skurski, P.; Rak, J.; Błażejowski, J. *J. Lumin.* **2003**, *105*, 27–34.
- (48) Koval'chuk, E. P.; Reshetnyak, O. V.; Chernyak, A. O.; Kovalyshyn, Ya. S. *Electrochim. Acta* **1999**, *44*, 4079–4086.
- (49) Arnold, J. S.; Browne, R. J.; Ogryzlo, E. A. *Photochem. Photobiol.* **1965**, *4*, 963–969.
- (50) Gray, E. W.; Ogryzlo, E. A. *Chem. Phys. Lett.* **1969**, *3*, 658–660.
- (51) Khan, A. U.; Kasha, M. *J. Am. Chem. Soc.* **1966**, *88*, 1574–1576.
- (52) Khan, A. U.; Kasha, M. *J. Am. Chem. Soc.* **1970**, *92*, 3293–3300.
- (53) Lewandowska-Andralojc, A.; Polyansky, D. E. *J. Phys. Chem. A* **2013**, *117*, 10311–10319.
- (54) Liang, C.; Wang, Z.-S.; Bruell, C. J. *Chemosphere* **2007**, *66*, 106–113.
- (55) House, D. A. *Chem. Rev.* **1962**, *62*, 185–203.
- (56) Yamashita, K.; Yamazaki-Nishida, S.; Harima, Y.; Segawa, A. *Anal. Chem.* **1991**, *63*, 872–876.
- (57) Gonzales-Velasco, J.; Rubinstein, I.; Crutchley, R. J.; Lever, A. B. P.; Bard, A. J. *Inorg. Chem.* **1983**, *22*, 822–825.